Journal of Nuclear Medicine, published on June 30, 2022 as doi:10.2967/jnumed.122.264329

Diagnostic accuracy of ^{99m}Tc-Sestamibi SPECT/CT for characterization of solid renal masses

Authors

Ashwin Singh Parihar*[1], Joyce Mhlanga*[1, 2], Carrie Ronstrom[2, 3], Lisa R. Schmidt[1], Robert S. Figenshau[2, 3], Farrokh Dehdashti*[1, 2], and Richard L. Wahl*[1, 2]

Affiliation

[1]Mallinckrodt Institute of Radiology, [2]Siteman Cancer Centre, and [3]Division of Urology, Department of Surgery, Washington University School of Medicine, Saint Louis, MO, USA.

*Contributed equally.

Word Counts

Total words: 4959

Tables: 5

Figures: 5 (3 – Main, 2 - Supplementary)

First Author

Ashwin Singh Parihar, M.B.B.S., M.D.
Postdoctoral Research Associate
Mallinckrodt Institute of Radiology, Washington University School of Medicine
4525 Scott Ave, MIR East Building, #3433
Saint Louis 63110, MO, USA
Email: ashwinp@wustl.edu; ORCID: 0000-0002-7983-4117

Corresponding Author

Richard L. Wahl, M.D.
Director: Mallinckrodt Institute of Radiology
510 South Kingshighway Boulevard
St. Louis, MO 63110
Email: rwahl@wustl.edu; ORCID: 0000-0002-7306-2590

Running Title

Sestamibi SPECT/CT for renal masses

Financial Support

None

ABSTRACT

Rationale

To assess the diagnostic accuracy of ^{99m}Tc-Sestamibi SPECT/CT for characterizing solid renal masses.

Methods

Imaging and clinical records of patients who underwent ^{99m}Tc-Sestamibi SPECT/CT for clinical work-up of their solid renal masses, from September 2018 to October 2021 were retrospectively reviewed. Histopathology formed the reference standard and the diagnoses were segregated as malignant/concerning (Renal cell carcinoma; RCCs other than chromophobe histology) and benign/non-concerning (oncocytic tumors including chromophobe RCC, other benign diagnoses) to calculate the sensitivity and specificity of ^{99m}Tc-Sestamibi SPECT/CT and contrast-enhanced CT (ceCT). The clinical reads of the SPECT/CT images were used for the visual classification of the lesions. Additionally, the SPECT images were manually segmented to obtain maximum and mean counts of the lesion, adjacent renal cortex, and maximum and mean lesion Hounsfield units (HU).

Results

^{99m}Tc-Sestamibi SPECT/CT was performed in 42 patients with 62 renal masses. A histopathologic diagnosis was available in 27 patients (18 men, 9 women), with 36 solid renal masses. ceCT findings were available in 20 of these patients. The most commonly identified single histology was clear-cell RCC (13/36; 36.1%). Oncocytic tumors were the most common group of non-concerning lesions (15/36) with oncocytoma as the predominant histology (n=6). The sensitivity and specificity of SPECT/CT for diagnosing a non-concerning lesion was 66.7%, and 89.5% respectively, compared to 10%, and 75% for ceCT, respectively. The lesion to kidney ratios for maximum and mean counts, and maximum lesion HU showed significant differences between the two groups ($P<0.05$). Lesion to kidney mean count ratio at a cut-off value of >0.46 showed a sensitivity and specificity of 87.5%, and 86.67% respectively for detecting non-concerning lesions which was significantly higher than that of ceCT.

Conclusion

The current literature on the utility of ^{99m}Tc-Sestamibi SPECT/CT for characterization of solid renal masses is limited. We offer additional evidence on the incremental value of ^{99m}Tc-Sestamibi SPECT/CT over ceCT for differentiating the malignant/aggressive renal tumors from the benign/indolent ones, thereby potentially avoiding over-treatment and its associated complications. Quantitative assessment can further increase the diagnostic accuracy of SPECT/CT and may be used in conjunction with the visual interpretation.

Key-words

^{99m}Tc-Sestamibi; MIBI; SPECT/CT; oncocytoma; chromophobe; renal cell carcinoma; renal mass; renal lesion

INTRODUCTION

The widespread utilization of cross-sectional imaging has led to an increased incidental detection of renal masses (*1*). Solid renal masses form a diagnostic challenge as conventional imaging with CT or MRI cannot reliably differentiate between the benign and indolent tumors from the more aggressive ones (*2*). Most of these tumors are malignant with clear-cell renal cell carcinoma (RCC) forming the most common histology, and around 10-20% are benign (*3*). The situation gets more complex with incidentally-detected small renal masses (≤4 cm in size) that are consistent with a clinical stage T1a RCC. These tumors were historically managed with universal radical nephrectomy. However it was recognized that the prognosis for patients with small renal masses is favorable, and a significant proportion of these patients can be managed with active surveillance (*4*,*5*). Further, among the 80% of these small renal masses that are malignant, only 20% are high-grade or locally invasive. The remaining majority have limited metastatic potential, including tumors such as chromophobe RCC (*4*,*6*).

The current recommendation for managing a small renal mass is to perform a biopsy whenever it is likely to change management, and a partial nephrectomy as the standard treatment whenever indicated (*7*). However, renal biopsy has technical challenges, including an around 20% non-diagnostic rate and a limited ability to differentiate low- and high-grade tumors (*8–10*). It is therefore clinically relevant and meaningful for a diagnostic test to not just distinguish benign from malignant tumors, but to differentiate the indolent tumors from the aggressive ones. This can help in potentially avoiding over-treatment in patients with relatively indolent tumors, while appropriately managing the more aggressive malignancies.

^{99m}Tc-Sestamibi is a lipophilic radiotracer that preferentially localizes in the mitochondria-rich cells. The benign/indolent renal tumors such as oncocytic neoplasms and chromophobe RCC are mitochondria-rich and typically avid on ^{99m}Tc-Sestamibi SPECT/CT compared to clear-cell RCC and other aggressive tumors that are typically non-avid (*11*). In addition, aggressive RCC's have a high multi-drug resistance pump expression that leads to active efflux of ^{99m}Tc-Sestamibi, thus contributing to negligible tracer retention (*12*). Prior studies have shown the effectiveness of ^{99m}Tc-Sestamibi in distinguishing

oncocytic tumors from the high-grade RCC (*11*,*13–16*). However, the data is still relatively sparse in terms of limited unique patient populations and the variety of benign and malignant histologies. A recent systematic review reported on four articles and mentioned the limited number of included studies as a major drawback (*17*). Additionally, there has been a limited emphasis on the quantitative aspects of SPECT/CT including parameters from both SPECT and CT components of the study. ^{99m}Tc-Sestamibi SPECT/CT is not yet currently recommended as an appropriate imaging for indeterminate renal masses by the American College of Radiology, which is largely due to the limited patient numbers in studies supporting its use (*18*).

Therefore, we conducted this study to assess the diagnostic accuracy of ^{99m}Tc-Sestamibi SPECT/CT for the characterization of the solid renal lesions as concerning or non-concerning, with histopathology as the reference standard in patients who had these scans for clinical indications. Secondary objectives included comparing the diagnostic performance of SPECT/CT with contrast-enhanced CT (ceCT), obtaining quantitative parameters on SPECT/CT and estimating their optimal cut-offs for differentiating between concerning and non-concerning renal lesions.

MATERIALS AND METHODS

Patients

Imaging and clinical records of patients who underwent ^{99m}Tc-Sestamibi SPECT/CT for the clinical evaluation of their solid renal lesions, from September 2018 to October 2021 were retrospectively reviewed. Histopathology results obtained either from biopsy or after surgical excision of the lesions formed the reference standard. Patients with no histopathology of their renal lesions were excluded from the study. The histopathologic diagnoses were segregated as “malignant/concerning” (RCCs other than chromophobe histology) and “benign/non-concerning” (oncocytic renal neoplasms, chromophobe RCC, other benign diagnoses) to calculate the sensitivity and specificity of ^{99m}Tc-Sestamibi SPECT/CT and ceCT. Considering that the majority of the benign/non-concerning neoplasms such as oncocytoma are positive on ^{99m}Tc-Sestamibi SPECT/CT, the sensitivity and specificity of both SPECT/CT and ceCT were calculated for the

diagnosis of a non-concerning neoplasm. Thus, the non-concerning lesions were regarded as 'positive' and concerning lesions were regarded as 'negative' for the estimation of diagnostic accuracy of SPECT/CT and ceCT.

^{99m}Tc-Sestamibi SPECT/CT

The patients were instructed to fast for approximately six hours prior to the radiotracer injection and to orally hydrate with ~500 mL of plain water prior to the study. The patients were injected intravenously with ~925 MBq (~25 mCi) ^{99m}Tc-Sestamibi. Approximately 75 minutes after the injection, SPECT/CT of the abdomen was acquired with the kidneys in the center of the long-axis field of view. A SPECT/ CT camera with low energy high-resolution collimator was used for imaging. The SPECT images were acquired with dual head with 3-degree stops using a 360-degrees clockwise rotation, matrix size of 128 x 128, 10 seconds per frame, step-and-shoot. The low-dose CT images were acquired for attenuation correction. The SPECT/CT images were reconstructed in trans-axial, sagittal and coronal views and interpreted by an experienced nuclear medicine physician. The interpreting physician was not blinded to the clinical information or to other imaging findings.

The lesions with a radiotracer uptake similar to or higher than the background renal parenchyma were considered positive on ^{99m}Tc-Sestamibi SPECT/CT, whereas those lesions that had a negligible radiotracer uptake, significantly lower than the background renal parenchyma were considered negative. Parameters such as size of the lesion, wall thickening, attenuation (HU), enhancement, internal septation, presence of fat, and calcification were taken into account for interpretation of the ceCT. The clinical reads of both ceCT and SPECT/CT were noted for the visual classification of the renal masses. Additionally, the SPECT/CT images were manually segmented to obtain maximum and mean counts of the lesion and adjacent renal cortex, and lesions maximum Hounsfield Units (HUmax) and mean Hounsfield Units (HUmean). Whole-lesion volumes of interest were used for calculating lesion counts and HU. A fixed 1.5 cm diameter spherical volume of interest was placed in the adjacent renal cortex, avoiding areas of high radiotracer activity (e.g. pelvi-calyceal system) for measuring the renal counts. The lesion-to-kidney count

ratios were calculated as Lesion:Kidney maximum counts (LKmax), and Lesion:Kidney mean counts (LKmean).

Statistical Analysis

The quantitative parameters (LKmax, LKmean, HUmax, HUmean) were tested for significant differences between the concerning and non-concerning lesions. Multiple logistic regression was utilized to build a model containing variables significant on univariate analyses. Receiving operator characteristic (ROC) curves were drawn to estimate the performance of quantitative SPECT. The ROC curves for visual and quantitative ^{99m}Tc-Sestamibi SPECT/CT and ceCT were compared using Hanley's method. Mann Whitney U-test (two-tailed) was used for comparing continuous variables between the visually-characterized concerning and non-concerning lesion groups. Fisher's exact test was used for comparing categorical variables between the two groups. Diagnostic accuracy of SPECT/CT and ceCT was expressed as sensitivity and specificity. A P value of <0.05 was regarded as significant.

The retrospective review was approved by the institutional review board, and the need for written informed consent was waived.

RESULTS

^{99m}Tc-Sestamibi was performed in 42 patients to evaluate their 62 renal lesions. 27 patients (18 male, 9 female) with 36 renal lesions had a final histopathologic diagnosis by either surgery (n=23) or biopsy (n=4). 20 of these patients also had a ceCT. The majority of the renal lesions (58.3%) were ≤4 cm in maximal axial dimension. Table 1 shows the clinical and demographic data of the study participants. The initial detection of the renal lesion(s) was incidental in 21/27 (77.8%) patients (19 – CT abdomen and pelvis, 2 – MRI abdomen).

Histopathology results showed 19 concerning (52.8%) and 17 non-concerning (47.2%) lesion diagnoses (Table 2). Overall, a clear-cell RCC was the most commonly identified single histology (13/36; 36.1%). As a group, oncocytic renal neoplasms (15/36; 41.6%) were most commonly diagnosed. The per-

lesion diagnostic test yield for providing a conclusive diagnosis (either true or false) was 84.6% (22/26) for CECT, and 94.4% (34/36) for SPECT/CT. Two lesions were most likely too small to be adequately characterized on ^{99m}Tc-Sestamibi SPECT/CT (maximal axial dimension of 0.8 cm and 1.5 cm, with final diagnosis of oncocytic renal neoplasm and chromophobe RCC, respectively). Of the four lesions where the ceCT findings were inconclusive, three were correctly diagnosed (two oncocytoma, one ccRCC) and one was a false positive (ccRCC on histopathology) on SPECT/CT.

Nine of 15 (60%) oncocytic renal neoplasms showed uptake on visual ^{99m}Tc-Sestamibi SPECT/CT and were correctly identified, while none (of the 10 masses with ceCT results) were correctly identified as non-concerning on ceCT. Four oncocytic renal neoplasms were incorrectly identified as concerning on SPECT/CT. Twelve of 13 ccRCC (92.3%) showed no tracer uptake on ^{99m}Tc-Sestamibi SPECT/CT and were correctly classified as concerning, while ceCT correctly classified 80% of these lesions (8 of 10 with ceCT results). ^{99m}Tc-Sestamibi SPECT/CT could correctly classify 80% of the papillary RCC (Figure 1) compared to 33.3% on ceCT. A patient with collision tumor (clear-cell and chromophobe RCC) was correctly classified on SPECT/CT and mis-classified as oncocytoma on ceCT (Figure 2). Table 3 shows the distribution of tumor histologies and their correctly identified proportions on ^{99m}Tc-Sestamibi SPECT/CT and ceCT.

Among the quantitative parameters, the lesion to kidney count ratios (LKmean and LKmax) were significantly higher in the non-concerning lesions compared to the concerning lesions (median LKmean 0.79 vs 0.26, P<0.001; median LKmax 0.95 vs 0.48, P=0.005) whereas the median HUmax was significantly lower in the non-concerning lesions (median HUmax 69 vs 90.5; P=0.01) (Table 4). There was no significant difference in the lesion size and HUmean between the concerning and non-concerning lesions. ROC curve analysis determined an optimal cut-off value of LKmax >0.64 (Area-under-the-curve; AUC 0.79; 95%CI:0.61-0.92; P<0.01) and LKmean >0.46 (AUC 0.85; 95%CI:0.67-0.95; P<0.0001) for detecting non-concerning lesions. There was no significant difference in the AUC of LKmax and LKmean based classifiers (P=0.18). Multiple logistic regression was used to analyze the relationship between

LKmean, HUmax and the detection of a non-concerning lesion. The odds of detecting a non-concerning lesion were higher with increasing LKmean (Odds ratio 271.65; 95%CI: 5.28-13981.9; P=0.005) and decreasing HUmax (Odds ratio 0.93; 95%CI: 0.87-0.99; P=0.019). The combination of these two quantitative measurements on logistics regression yielded an AUC of 0.92 (95%CI: 0.76-0.99). Visually interpreted ^{99m}Tc-Sestamibi SPECT/CT had a sensitivity and specificity of 66.7% (95%CI: 38.4-88.2) and 89.5% (95%CI: 66.7-98.7), respectively. This was not significantly different from the performance of ceCT (Table 5, Supplementary Figure 1). However, quantitative SPECT/CT (based on a LKmean cut-off of >0.46 for a non-concerning lesion – Supplementary Figure 2) performed significantly better (AUC 0.85; 95%CI:0.62-0.96) than ceCT (AUC 0.57; 95%CI: 0.34-0.78) with a P=0.023.

DISCUSSION

^{99m}Tc-Sestamibi SPECT/CT on visual interpretation correctly identified 89.5% of all aggressive tumors and 60% of all the oncocytic neoplasms in our study. The false positive results (a concerning lesion labeled as non-concerning) stemmed from tracer avidity in two concerning lesions that were positive based on the quantitative criteria as well (Clear-cell RCC with LKmean of 1.17, and papillary RCC with LKmean of 0.82). A few prior studies have also shown that a limited number of papillary and clear-cell RCC may show uptake of ^{99m}Tc-Sestamibi (*14,16*). This is likely related to a higher contribution from the mitochondrial content of these tumors and a relatively lower expression of the multi-drug resistance protein. Although a prior study showed that papillary RCC have a uniformly higher multi-drug resistance protein expression in comparison to mitochondrial content, this might not hold true in a larger cohort (*12*).

Our study had a lower detection rate of the non-concerning lesions on visual ^{99m}Tc-Sestamibi SPECT/CT compared to the prior studies. One possible reason is the relatively higher number of benign/non-concerning lesions included in our study (~ 47%) compared to the prior ones (~ 24%) (*15–17*). Because of the higher number of non-concerning lesions, we could report that oncocytomas may not universally show a high radiotracer uptake on ^{99m}Tc-Sestamibi SPECT/CT and can be missed on both visual and quantitative assessment (Figure 3). However, in two of the three cases where a visual assessment was

false negative and a quantitative assessment was performed, the latter was able to make the correct diagnosis. Since the pattern of radiotracer uptake can vary widely in the oncocytic tumors, ranging from homogeneously increased uptake compared to the normal renal parenchyma to areas of low-grade patchy uptake with interspersed photopenia, quantitative assessment with the lesion to background count ratios can complement visual interpretation (*19*).

Most prior studies have utilized either a visual interpretation alone or a combination of visual interpretation with a ratio of lesion to kidney maximum counts. Our LKmax cut-off of >0.64 for detecting non-concerning lesions is similar to that reported previously, which validates the utility of this quantitative criterion (*11*,*20*). We additionally introduced a lesion-to-kidney mean count ratio (LKmean) which is more reflective of the count distribution in the entire tumor compared to the total counts in a heterogeneous lesion. We also propose combining the HUmax and LKmean on SPECT/CT that showed a higher AUC of 0.92 (95%CI: 0.76-0.99) than the other quantitative parameters alone on the ROC analyses. Although this method did not show a statistically significant difference from using LKmean alone, it is quite possibly related to the relatively low number of lesions included in this study. The utilization of quantitative parameters from both SPECT and CT components has not been explored before and needs validation in future prospective studies. The prospects of performing a single ^{99m}Tc-Sestamibi SPECT/ceCT may also be explored as a one-stop shop for evaluation of the renal masses (*21*). This can reduce the number of patient visits and potentially improve interpretation of the renal masses by combining features from both SPECT and ceCT.

It is recognized that conventional imaging such as CT and MRI often detect renal lesions incidentally, but cannot reliably distinguish indolent renal tumors from aggressive ones. In our study, 9/15 oncocytic lesions were correctly identified on SPECT/CT, whereas none could be accurately categorized on ceCT. Although the difference in sensitivity and specificity of visually interpreted SPECT/CT and ceCT was not statistically significant, it is likely due to the limited number of lesions studied by both modalities. The incremental value of SPECT/CT in detecting the oncocytic lesions is clinically relevant and can

potentially avoid overtreatment in these patients. A prior study has shown that addition of ^{99m}Tc-Sestamibi SPECT/CT after conventional imaging increases the diagnostic confidence and improves the accuracy of differentiating benign from malignant tumors (*20*). Further, ^{99m}Tc-Sestamibi SPECT/CT followed by biopsy to confirm benign small renal masses is a reported to be a cost-effective strategy with the highest probability of not over-treating the benign tumors and appropriately treating the malignant ones (*22*).

Our study has its limitations. These include a retrospective design with a limited number of included participants, leading to wide confidence-intervals in estimates of diagnostic accuracy, although we have several unique histologic types where we could show the differences in performance of ceCT and ^{99m}Tc-Sestamibi SPECT/CT. The diagnostic accuracy of both ceCT and ^{99m}Tc-Sestamibi SPECT/CT is possibly under-estimated due to the retrospective design where SPECT/CT was more likely to be performed in challenging cases with lack of a reliable, conclusive diagnosis on ceCT. Nevertheless, the literature is still quite sparse in this space in terms of original articles describing findings in unique populations (*11*,*13*–*16*). Since we excluded patients with no histopathology results, this might have led to selective exclusion of a higher number of benign/non-concerning lesions that were more likely to be managed clinically by follow-up imaging instead of an active intervention. We hope to follow up our patients to determine how many lesions were stable over time without intervention. However, our stringent inclusion criteria with histopathology as the reference standard helped form a robust comparison for both ceCT and SPECT/CT. Additionally, most patients in our study had surgical histopathology results, thereby minimizing the potential inconclusive and/or false results with a biopsy. Instead of central reads, we incorporated both the clinical visual reads and quantitative results for SPECT/CT, which is likely better reflective of the real-world scenario. The cut-offs for mean and maximum count ratio between the lesions and the normal renal parenchyma were set post-hoc, and these would need prospective validation in larger cohorts. Importantly we combined the quantitative information from SPECT and CT, in terms of count ratios and HUmax, which performed better than either of these parameters alone. Future prospective studies can focus on the

utilization of these parameters along with the visual reads to improve the diagnostic accuracy of ^{99m}Tc-Sestamibi SPECT/CT.

CONCLUSION

The current literature on the utility of ^{99m}Tc-Sestamibi SPECT/CT for characterization of solid renal masses is very limited, with a recently published systematic review reporting only four studies. We provide additional evidence on the utility of ^{99m}Tc-Sestamibi SPECT/CT especially in patients with an inconclusive ceCT for differentiating the malignant/aggressive renal tumors from the benign/indolent ones, therefore potentially avoiding over-treatment and its associated complications in the latter category. Quantitative assessment can further increase the diagnostic accuracy of SPECT/CT and may be used in conjunction with the visual interpretation.

ACKNOWLEDGEMENTS

None

DISCLOSURE

No potential conflicts of interest relevant to this article exist.

KEY-POINTS

QUESTION: What is the diagnostic accuracy of ^{99m}Tc-Sestamibi SPECT/CT for solid renal lesions?

PERTINENT FINDINGS: In this retrospective study, we showed that ^{99m}Tc-Sestamibi SPECT/CT had a sensitivity and specificity of 66.7% and 89.5% respectively for diagnosing a non-concerning solid renal lesion.

IMPLICATIONS FOR PATIENT CARE: The study shows that ^{99m}Tc-Sestamibi SPECT/CT can aid in the diagnosis of solid renal lesions, especially in cases where the ceCT results are inconclusive.

REFERENCES

1. Welch HG, Skinner JS, Schroeck FR, Zhou W, Black WC. Regional variation of computed tomographic imaging in the United States and the risk of nephrectomy. *JAMA Intern Med*. 2018;178:221-227.

2. Silverman SG, Israel GM, Herts BR, Richie JP. Management of the incidental renal mass. *Radiology*. 2008;249:16-31.

3. Frank I, Blute ML, Cheville JC, Lohse CM, Weaver AL, Zincke H. Solid renal tumors: An analysis of pathological features related to tumor size. *J Urol*. 2003;170:2217-2220.

4. Sanchez A, Feldman AS, Ari Hakimi A. Current management of small renal masses, including patient selection, renal tumor biopsy, active surveillance, and thermal ablation. *J Clin Oncol*. 2018;36:3591-3600.

5. Pierorazio PM, Johnson MH, Ball MW, et al. Five-year analysis of a multi-institutional prospective clinical trial of delayed intervention and surveillance for small renal masses: The DISSRM registry. *Eur Urol*. 2015;68:408-415.

6. Jewett MAS, Richard PO, Finelli A. Management of small renal mass: An opportunity to address a growing problem in early stage kidney cancer. *Eur Urol*. 2015;68:416-417.

7. Finelli A, Ismaila N, Bro B, et al. Management of small renal masses: American society of clinical oncology clinical practice guideline. *J Clin Oncol*. 2017;35:668-680.

8. Menogue SR, O'Brien BA, Brown AL, Cohen RJ. Percutaneous core biopsy of small renal mass lesions: A diagnostic tool to better stratify patients for surgical intervention. *BJU Int*. 2013;111.

9. Leveridge MJ, Finelli A, Kachura JR, et al. Outcomes of small renal mass needle core biopsy, nondiagnostic percutaneous biopsy, and the role of repeat biopsy. *Eur Urol*. 2011;60:578-584.

10. Ball MW, Bezerra SM, Gorin MA, et al. Grade heterogeneity in small renal masses: Potential implications for renal mass biopsy. *J Urol*. 2015;193:36-40.

11. Gorin MA, Rowe SP, Baras AS, et al. Prospective evaluation of 99mTc-sestamibi SPECT/CT for the diagnosis of renal oncocytomas and hybrid oncocytic/chromophobe tumors. *Eur Urol*. 2016;69:413-416.

12. Rowe SP, Gorin MA, Solnes LB, et al. Correlation of 99mTc-sestamibi uptake in renal masses with mitochondrial content and multi-drug resistance pump expression. *EJNMMI Res*. 2017;7:80.

13. Rowe SP, Gorin MA, Gordetsky J, et al. Initial experience using 99mTc-MIBI SPECT/CT for the differentiation of oncocytoma from renal cell carcinoma. *Clin Nucl Med*. 2015;40:309-313.

14. Tzortzakakis A, Gustafsson O, Karlsson M, Ekström-Ehn L, Ghaffarpour R, Axelsson R. Visual evaluation and differentiation of renal oncocytomas from renal cell carcinomas by means of 99mTc-sestamibi SPECT/CT. *EJNMMI Res*. 2017;7:29.

15. Sistani G, Bjazevic J, Kassam Z, Romsa J, Pautler S. The value of 99mTc-sestamibi single-photon emission computed tomography-computed tomography in the evaluation and risk stratification of renal masses. *Can Urol Assoc J*. 2020;15:197-201.

16. Zhu H, Yang B, Dong A, et al. Dual-Phase 99mTc-MIBI SPECT/CT in the characterization of enhancing solid renal tumors: A single-institution study of 147 Cases. *Clin Nucl Med*. 2020;45:765-770.

17. Wilson MP, Katlariwala P, Murad MH, Abele J, McInnes MDF, Low G. Diagnostic accuracy of 99mTc-sestamibi SPECT/CT for detecting renal oncocytomas and other benign renal lesions: a systematic review and meta-analysis. *Abdom Radiol*. 2020;45:2532-2541.

18. Wang ZJ, Nikolaidis P, Khatri G, et al. ACR Appropriateness Criteria® Indeterminate Renal Mass. *J Am Coll Radiol*. 2020;17:S415-S428.

19. Campbell SP, Tzortzakakis A, Javadi MS, et al. 99m Tc-sestamibi SPECT/CT for the characterization of renal masses: a pictorial guide. *Br J Radiol*. 2018;91:20170526.

20. Sheikhbahaei S, Jones CS, Porter KK, et al. Defining the added value of 99mTc-MIBI SPECT/CT to conventional cross-sectional imaging in the characterization of enhancing solid renal masses. *Clin Nucl Med*. 2017;42:e188-e193.

21. Israel O, Pellet O, Biassoni L, et al. Two decades of SPECT/CT – the coming of age of a technology: An updated review of literature evidence. *Eur J Nucl Med Mol Imaging*. 2019;46:1990-2012.

22. Su ZT, Patel HD, Huang MM, et al. Cost-effectiveness analysis of 99mTc-sestamibi SPECT/CT to guide management of small renal masses. *Eur Urol Focus*. 2021;7:827-834.

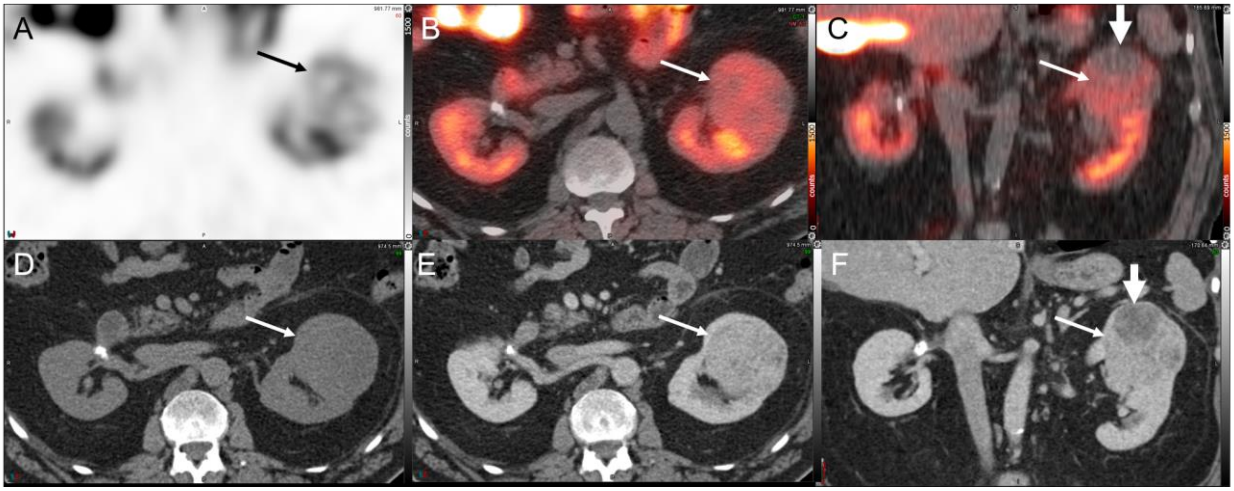

Figure 1 – 67 year-old man with previously diagnosed right renal-cell carcinoma (RCC), post right partial nephrectomy presented with an enlarging left renal mass. ^{99m}Tc-Sestamibi axial SPECT (A), and fused SPECT/CT (axial – B, coronal - C) images show a mass in the superior pole of the left kidney with its inferior part showing tracer avidity (thin-arrow) and the superior part showing relative photopenia (thick-arrow). It was diagnosed as a likely collision tumor on SPECT/CT with the inferior, tracer-avid region likely representing an oncocytic tumor and the superior, photopenic region likely a concerning RCC. ceCT images (non-contrast – D, post-contrast nephrogenic phase axial – E, coronal - F) showed a solid heterogeneously enhancing left renal mass likely representing oncocytoma. The patient underwent left partial robot-assisted laparoscopic nephrectomy and the histopathology showed a collision tumor composed of clear cell RCC (rhabdoid differentiation, WHO/ISUP grade 4) and an eosinophilic variant of chromophobe RCC.

Figure 2 – A 53 year-old woman with a right interpolar mass underwent a MRI that suggested an oncocytoma or chromophobe RCC. ^{99m}Tc-Sestamibi SPECT/CT was performed a week later. Axial SPECT (A), CT (B) and fused SPECT/CT images (C) showed an exophytic renal mass in the right interpolar region (arrow) with negligible tracer uptake that was suggestive of a concerning RCC. The patient underwent right partial robot-assisted laparoscopic nephrectomy and the histopathology was consistent with a papillary RCC (WHO/ISUP grade 2).

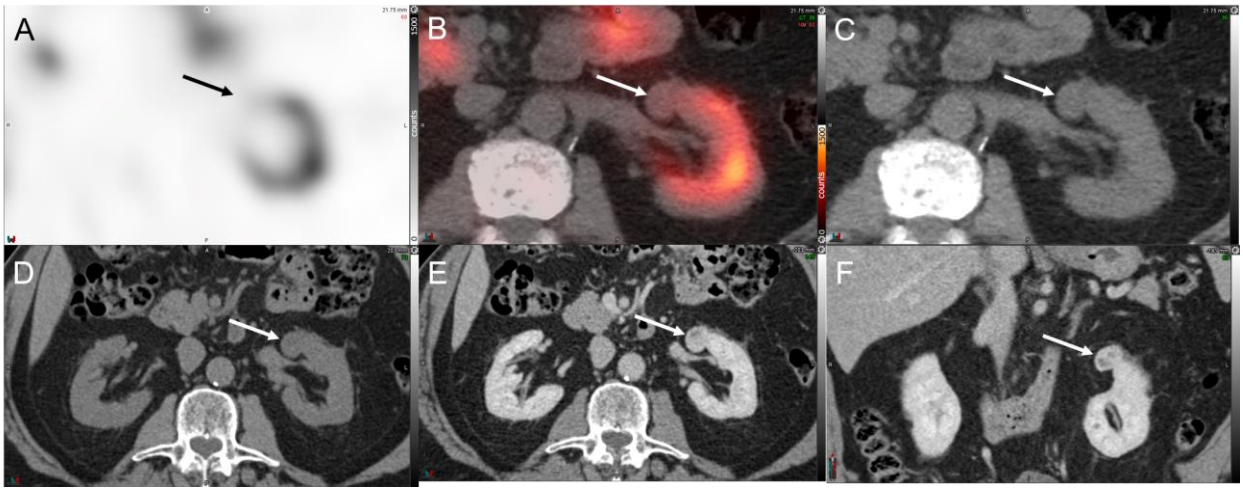

Figure 3 – 77 year-old man presented with a left renal mass. ^{99m}Tc-Sestamibi axial SPECT (A), fused SPECT/CT (B) and CT (C) images show an exophytic mass in the anterior inter-polar region of the left kidney (arrow) with negligible tracer uptake, likely representing a concerning RCC. The maximum and mean lesion-to-kidney count ratios were both 0.3 for this lesion. ceCT images (axial, non-contrast – D, post-contrast nephrogenic phase – E, coronal - F) showed enhancement in the mass and also suggested the diagnosis of a RCC. The patient underwent left partial robot-assisted laparoscopic nephrectomy and the histopathology was consistent with oncocytoma.

Table 1 – Demographic and clinical data of the study participants

Parameter	Value
Number of patients	27 (Male - 18, Female - 9)
Age in years, median (interquartile range)	68 (58.5-77)
Procedure for histopathologic analysis	Surgical histopathology – 23 (Partial nephrectomy – 17; Radical nephrectomy - 6); Biopsy - 4
Number of renal lesions with histopathology, stratified by maximum dimension	Total – n=36 (100%) ≤4 cm – n=21 (58.3%) >4, ≤7 cm – n=13 (36.1%) >7, ≤10 cm – n=2 (5.5%)
Maximum dimension of the lesion in cm, median (interquartile range)	3.3 (2.07-4.57)
Tumor laterality, n (%)	Left – 19 (52.8%); Right – 17 (47.2%)
Duration between ceCT and SPECT/CT in days, median (interquartile range)	30 (19.5-70.5)

371 **Table 2 – Histopathologic diagnosis of the renal lesions stratified by size on imaging**

Diagnosis category	Histopathology	Maximum axial dimension of lesion on imaging		
		≤4 cm (n=21)	>4, ≤7 cm (n=13)	>7, ≤10 cm (n=2)
Concerning histopathology	Clear cell RCC	6 (28.6%)	6 (46.1%)	1 (50%)
	Papillary RCC	4 (19%)	1 (7.7%)	0 (0%)
	Collision clear-cell, chromophobe RCC	0 (0%)	1 (7.7%)	0 (0%)
Non concerning histopathology	Oncocytoma	4 (19%)	1 (7.7%)	1 (50%)
	Chromophobe RCC	1 (4.8%)	1 (7.7%)	0 (0%)
	Hybrid oncocytic chromophobe tumor	1 (4.8%)	1 (7.7%)	0 (0%)
	Oncocytic renal neoplasm	3 (14.3%)	1 (7.7%)	0 (0%)
	RCC with oncocytic features	0 (0%)	1 (7.7%)	0 (0%)
	Angiomyolipoma	2 (9.5%)	0 (0%)	0 (0%)

372

373

Table 3 – Distribution of tumor histologies and their correctly identified proportions on ^{99m}Tc-Sestamibi SPECT/CT and ceCT

Histologic type		Histopathology, n (%)	Correct diagnosis on ^{99m}Tc-Sestamibi SPECT/CT, n (%)	Correct diagnosis on ceCT, n (% of lesions where ceCT was performed)
Concerning histopathology	Clear cell RCC	13 (36.1%)	12 (92.3%)	8 (8/10; 80%)
	Papillary RCC	5 (13.9%)	4 (80%)	1 (1/3; 33.3%)
	Collision clear-cell, chromophobe RCC	1 (2.8%)	1 (100%)	0 (0/1; 0%)
Non-concerning histopathology	Oncocytoma	6 (16.7%)	3 (50%)	0 (0/4; 0%)
	Chromophobe RCC	2 (5.5%)	1 (50%)	0 (0/2; 0%)
	Hybrid oncocytic chromophobe tumor	2 (5.5%)	2 (100%)	0 (0/0; 0%)
	Oncocytic renal neoplasm	4 (11.1%)	2 (50%)	0 (0/3; 0%)
	RCC with oncocytic features	1 (2.8%)	1 (100%)	0 (0/1; 0%)
	Angiomyolipoma	2 (5.5%)	1 (50%)	1 (1/2; 50%)

Table 4 - Comparison of quantitative parameters on ^{99m}Tc-Sestamibi SPECT/CT for differentiating clinically concerning and non-concerning renal lesions

Quantitative parameters	Concerning lesions	Non-concerning lesions	P value
Lesional maximal axial dimension in cm (median, IQR)	3.3 (2.3-4.8)	2.95 (1.47-4.62)	0.386
Lesion to kidney ratio - maximum counts (median, IQR)	0.48 (0.37-0.64)	0.95 (0.69-1.04)	**0.005**
Lesion to kidney ratio - mean counts (median, IQR)	0.26 (0.12-0.43)	0.79 (0.55-0.99)	**<0.001**
Lesion – maximum HU (median, IQR)	90.5 (78-101)	69 (60.5-89.5)	**0.016**
Lesion – mean HU (median, IQR)	26.25 (22.98-31.75)	28.1 (23.55-31.0)	0.801

Table 5 – Comparison of diagnostic accuracy of ^{99m}Tc-Sestamibi SPECT/CT and ceCT for diagnosing a non-concerning renal lesion

Diagnostic modality	TP (n)	TN (n)	FP (n)	FN (n)	Sensitivity (95%CI)	Specificity (95%CI)
^{99m}Tc-Sestamibi SPECT/CT – visual interpretation	10	17	2	5	66.7 (0.38-0.88)	89.47 (0.67-0.99)
ceCT	1	9	3	9	10.0 (0.25-0.44)	75.0 (0.43-0.95)
^{99m}Tc-Sestamibi SPECT/CT – Lesion to kidney count ratio (mean)*	14	13	2	2	87.5 (0.62-0.98)	86.67 (0.59-0.98)

*Using cut-off value of LKmean > 0.46 for a non-concerning lesion. TP – True Positive, TN – True Negative, FP – False Positive, FN – False Negative; Note that non-concerning lesions are positive, and concerning lesions are negative.

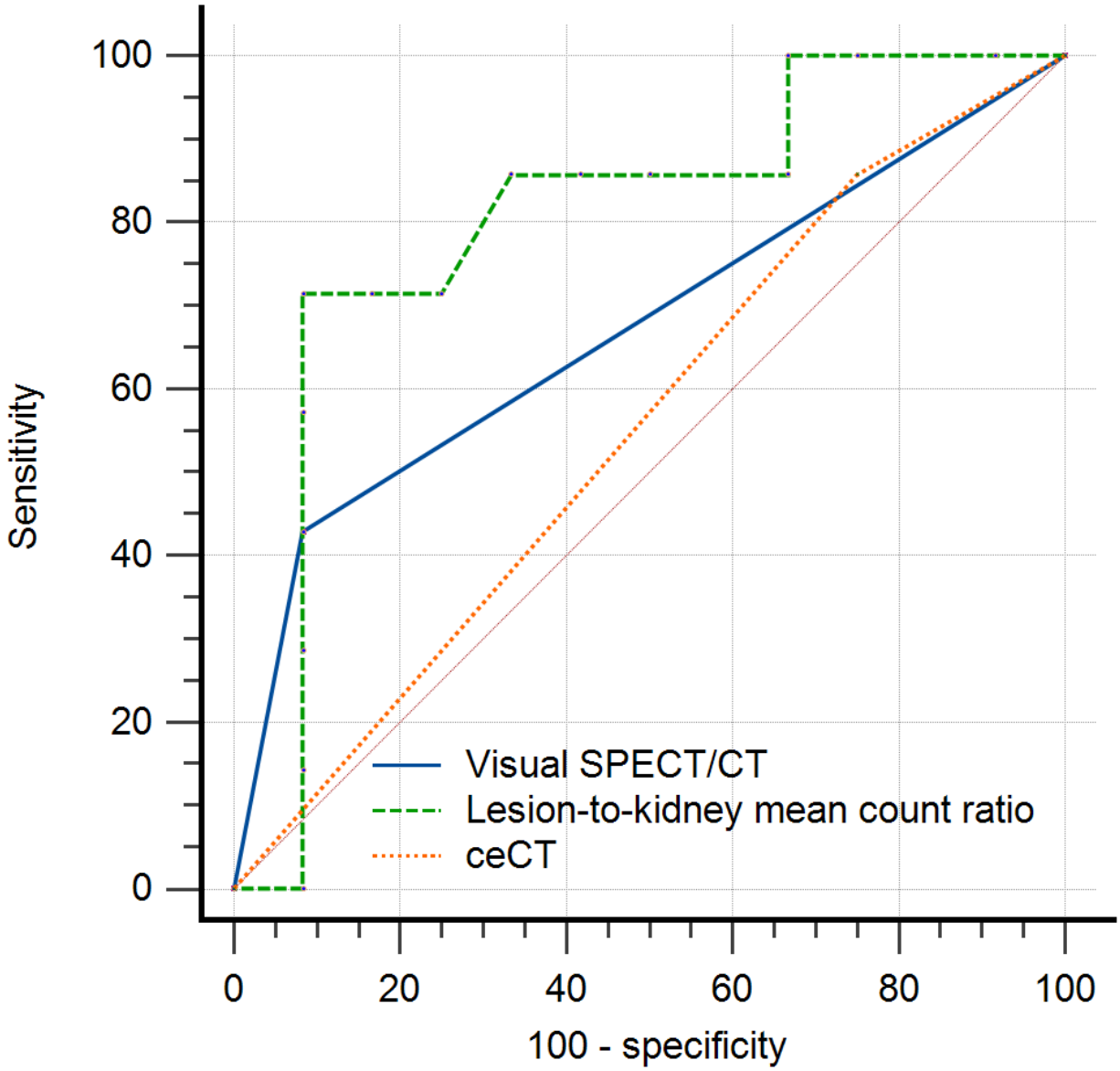

388

389 **Supplementary Figure 1** – Receiver operating characteristic (ROC) curves comparing the performance of
390 quantitative (lesion-to-kidney mean count ratio; LKmean) SPECT/CT, visual SPECT/CT and ceCT for
391 correctly diagnosing non-concerning renal masses showed the highest area under the curve with the
392 quantitative SPECT/CT (AUC=0.80) followed by visual SPECT/CT (0.67) and ceCT (0.55), although the
393 differences were not statistically significant (P>0.05).

394

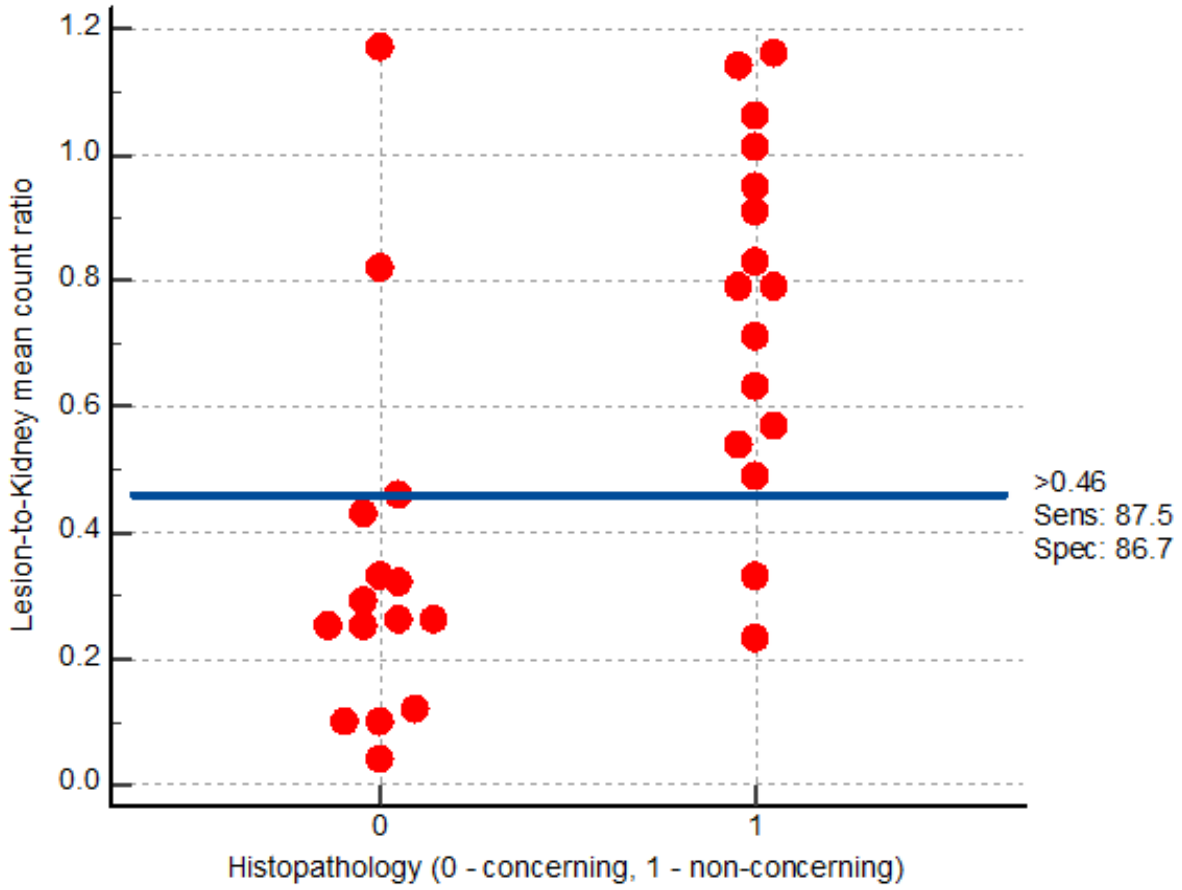

395

396 **Supplementary Figure 2** – Dot diagram showing the segregation of lesions as concerning vs non-
397 concerning using LKmean with a cut-off value of >0.46 for a non-concerning lesion.

398

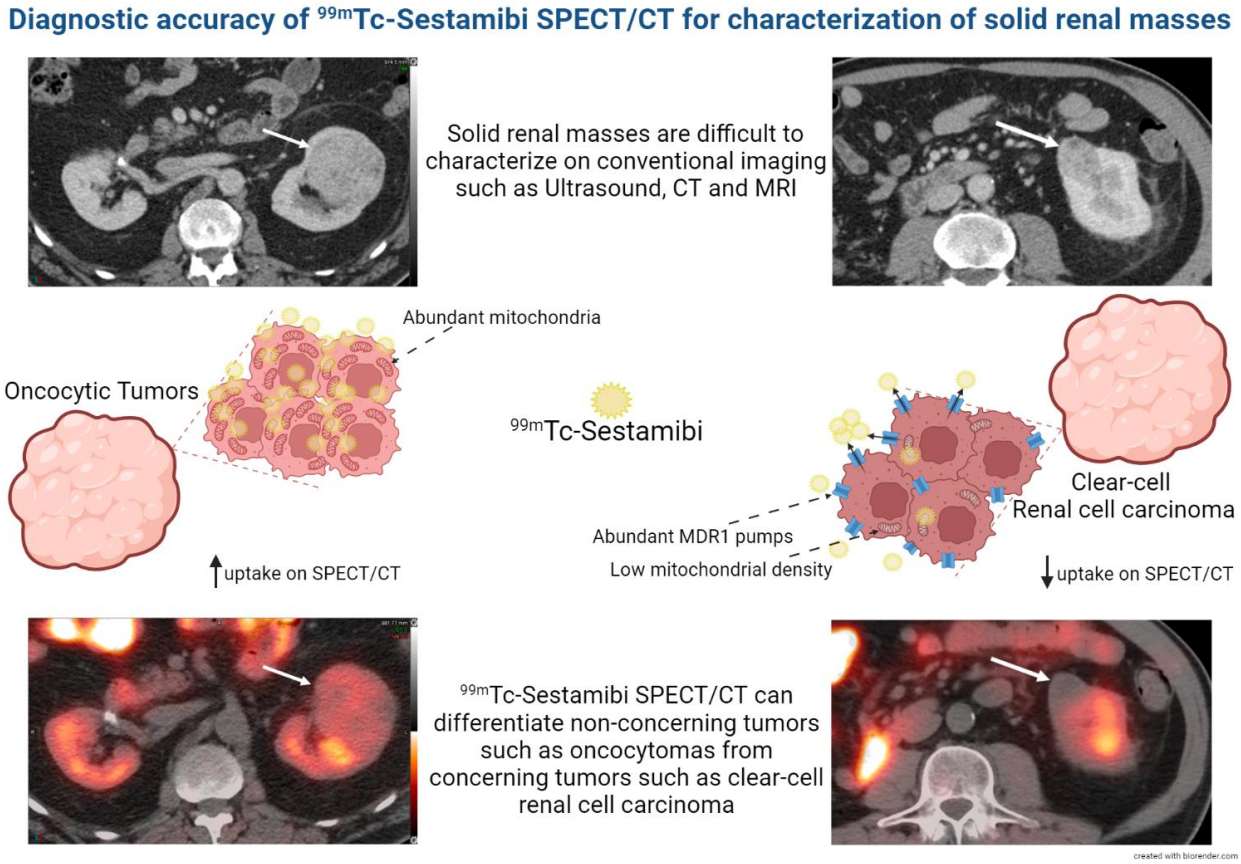

399

400 **Graphical Abstract**